Published in final edited form as:

J Am Chem Soc. 2019 October 23; 141(42): 16544–16547. doi:10.1021/jacs.9b05978.

Photorelease of 2-Arachidonoylglycerol in Live Cells

Aurélien Laguerre[†], **Sebastian Hauke**[‡], **Jian Qiu**[†], **Martin J. Kelly**[†], **Carsten Schultz**[*,†,‡]

[†]Department of Chemical Physiology & Biochemistry, OHSU, Portland, Oregon, United States

[‡]European Molecular Biology Laboratory, Cell Biology and Biophysics Unit, 69117 Heidelberg, Germany

Abstract

2-Arachidonoylglycerol (2-AG) is acting as a full agonist of cannabinoid receptor 1 and 2. Direct manipulation of 2-AG levels is a challenging task. The amphiphilic properties and the instability of 2-AG in aqueous media complicate its use as a drug-like molecule. Additionally, inhibition of the protein machinery that regulates 2-AG levels may also affect other monoacylglycerols. Therefore, we developed a novel method to elevate 2-AG levels with a flash of light. The resulting tool is a photoactivatable "caged" 2-arachidonoylglycerol (cg2-AG) allowing for the rapid photorelease of the signaling lipid in live cells. We characterized the mechanism of uncaging and the effect of 2-AG on the regulation of the β-cell signaling network. After uncaging of 2-AG, we monitored calcium levels, CB1-GIRK channel coupling, and CB1-mediated inhibition of adenylate cyclase and protein kinase A activity.

The endocannabinoid lipids anandamide and 2-arachidonoylglycerol (2-AG) stimulate the two G-protein coupled cannabinoid receptor subtypes 1 and 2 (CB1 and CB2).[1,2] The downstream signaling network regulates a multitude of processes such as mood, appetite, pain sensation, memory, and insulin secretion.[3,4] 2-AG is produced on demand via the activation of diacylglycerol lipases α and β but also depends on the dephosphorylation of lysophosphatidic acid to 2-AG. 2-AG levels are further regulated by several monoacylglycerol lipases (MAGL, ABHD6, and ABHD12) that degrade 2-AG into glycerol and arachidonic acid.[5] All three enzyme are located at the plasma membrane, but MAGL also resides in the cytosol.[6] 2-AG likely targets its receptors in the producing cell as well as triggering CB1 and CB2 in neighboring cells.[7] CB1 and CB2 not only act via the trimeric Gi/o protein but also open the G protein-coupled inwardly rectifying potassium channel (GIRK) via the G-protein β/γ subunit.[8] The physicochemical properties of 2-AG complicate its use as a drug-like molecule for external administration, due to its amphiphilic properties, its low solubility in aqueous solutions, and its fast molecular rearrangement thermodynamically favoring the formation of the primary ester in 1(3)-AG.[9] As a result,

[*]**Corresponding Author** schulcar@ohsu.edu.

ASSOCIATED CONTENT

Supporting Information

The Supporting Information is available free of charge on the ACSPublicationswebsite at DOI: 10.1021/jacs.9b05978.

Figures S1–S14, experimental details, characterization data, NMR spectra (PDF)

The authors declare no competing financial interest.

commercially available 2-AG is composed of a 9:1 ratio of the two isomers. Therefore, a strategy that prevents premature isomerization will be beneficial. Other strategies to manipulate endogenous 2-AG levels make use of lipase inhibitors, albeit in an unspecific fashion.[10] Effects on other monoacylglycerols may activate undesired protein targets and complicate the interpretation of experimental observations. A more direct approach is the use of caged lipids, which offer a unique spatiotemporal precision to release natural lipids inside the cell, with a simple flash of light.[11] Caged lipids possess a photoremovable protecting group (PRPG) covalently attached to one of the crucial functional groups of the lipid, thereby preventing its recognition by the cellular machinery. A flash of UV light is sufficient for the PRPG to release the signaling molecule. Here, this concept is applied to 2-AG, allowing the exclusive manipulation of 2-AG levels and its downstream effectors with high spatiotemporal resolution without interfering with the genetic or the protein machinery. We monitored calcium levels and CB1-mediated inhibition of adenylate cyclase and protein kinase A activity via confocal microscopy as well as CB1-GIRK channel coupling by electrophysiology. It should be mentioned that, for activating CB1, Westphal et al. recently prepared and tested photoswitchable tetrahydrocannabinol derivatives.[12] Herein, we aimed at stimulating the cannabinoid receptors by its endogenous ligand, which required the ability to selectively manipulate 2-AG concentration in live cells.

PRPGs such as nitrobenzyl groups and coumarins have been widely used to prepare “caged” lipid derivatives.[13–15] However, the protection of 1,3-diols has been a difficult task. Previous attempts described by the Lawrence group showed that six-membered ring acetals formed with 6-bromo-7-hydroxy-4-formylcoumarin were resistant to photocleavage.[16] We hypothesized that the presence of an ester on the six-membered ring of the acetal of caged 2-AG (cg2-AG) would reduce the electron density on the oxygen-bearing glycerol leaving group. We investigated 7-diethylamino coumarin as a scaffold for caging 2-AG. Its fluorescent properties allow for the visualization in single cells prior to photolysis. Unlike with classic caging strategies, the uncaging mechanism of photosensitive cyclic acetals would impose the departure of a chemically altered chromophore after illumination providing the opportunity to follow the uncaging process by simply monitoring changes in fluorescence emission. A short and straightforward synthetic pathway allowed for the synthesis of cg2-AG in only four steps (Figure 1A). The first synthetic steps were directly inspired by the described synthesis of the 7-diethylamino-4-hydroxymethyl-coumarin.[17] 7-Diethylamino-4-formyl-coumarin **3** was used for acetal formation with glycerol. Alcohol 4 provided a versatile platform for the attachment of fatty acids and was used to couple arachidonic acid, thereby providing cg2-AG.

Our first attempts to characterize the uncaging of cg2-AG in organic solvents such as chloroform, dimethyl sulfoxide, ethanol, or methanol were unsuccessful. Using a 1 kW xenon lamp equipped with a 350 nm long-pass filter, nuclear magnetic resonance experiments showed that cg2-AG was photoresistant in organic solvents even after 15 min of irradiation (Figure S6). Following the release mechanism proposed by Lawrence and co-workers,[16] we hypothesized that the presence of water could be a requirement for proper uncaging. Satisfactorily, liquid chromatography/mass spectrometry (LC/MS) analysis of a 10 μM aqueous solution confirmed the photorelease of 2-AG in water (Figures S7 and S8).

Further UV/vis HPLC analysis demonstrated the photorelease of intermediate **3** and its hydrated form as well as 2-AG (Figure S9).

We confirmed that the caged lipid did not precipitate over time. UV irradiation had a strong effect on the sample, triggering a rapid and drastic reduction of the absorbance (Figure 1C). Fluorescence emission intensity measurements of cg2-AG under the same conditions showed the same tendency (Figure 1D, Figure S9). Prolonged light exposure resulted in a stable fluorescence intensity, indicating that the photoreaction came to completion and produced a new photostable compound (Figure S10C and S10D). While the expected aldehyde **3** is highly fluorescent (Figure S9E), we identified the hydrate of **3** as the low-fluorescent species (Figure S9F). It should be mentioned that, in cells, the formation of Schiff's bases and glutathione adducts might contribute to the observed reduction in fluorescence.[13] Similar experiments in ethanol showed no fluorescence decrease of the caged compound after illumination (Figure S11C), further indicating the essential participation of water molecules in the uncaging mechanism. To confirm our hypothesis that the ester would reduce the electron density and encourage the departure of the leaving group, the experiments were performed with alcohol **4** (Figure 1A–C). The absorbance of **4** was red-shifted toward lower energy wavelengths (401 nm vs 389 nm for cg2-AG) and a Stokes shift of 103 nm (vs 87 nm for cg2-AG), demonstrating the electron-withdrawing effect of the ester. As expected from Lawrence's work, illumination at 350 nm did not affect the UV/vis absorbance and fluorescence emission intensity of **4** (Figures 1C and S11B).

The mouse β-cell line MIN6 is known to endogenously express CB1 and CB2 and served as a model for studying photoactivation of cg2-AG and its effect on cannabinoid receptors in live cells.[18] The insertion of a lipophilic PRPG onto both hydroxyl groups of the glycerol decreased the amphiphilic nature of 2-AG, prohibited migration of the fatty acid, and facilitated the cellular internalization of the caged compound leading to rapid and complete cellular accumulation of cg-2AG in internal membranes at 1 to 10 μM extracellular concentration (Figure S12). As previously observed in vitro, flash photolysis at 375 nm in live MIN6 β-cells triggered a strong decrease (62.0%, $n = 25$) of the fluorescence emission intensity (Figures 1B and S12A). Illumination of control alcohol **4** (Figure 1B) was ineffective. Unlike many other diethyl amino-coumarin cages, cg2-AG was almost completely resistant to photolysis at 405 nm in cells (Figure S12B). This feature allowed monitoring the amount of caged lipid by confocal microscopy with 405 nm illumination during the experiment without triggering uncaging. At 375 nm, we followed the release of the monoacylglycerol by directly measuring the drop in fluorescence intensity at a single cell level.

Endocannabinoid lipids are known to induce a transient elevation of intracellular Ca^{2+} levels ($[Ca^{2+}]_i$) through activation of CB1.[19] Accordingly, MIN6 cells in the presence of 11 mM glucose at 37 °C were treated with permeant cg2AG (10 μM) as well as the calcium indicator Fluo-4/AM (5 μM) for 20 min. Fluctuations of $[Ca^{2+}]_i$ were monitored through excitation at 488 nm and emission above 515 nm (F/F_0) on the confocal microscope. A clear and transient elevation of the intracellular calcium concentration $[Ca^{2+}]_i$ was observed among the illuminated cells ([cg2-AG] = 10 μM, $n = 136$ cells), characteristic of the activation of CB1 (Figures 2A and S13) and in agreement with reports made by other

groups.[7,9,17,18] This transient was almost completely abolished when cells were preincubated with the CB1 antagonist rimonabant (1 μM; [cg2-AG] = 10 μM, n = 79 cells), confirming the specific activation of the CB1 receptor upon uncaging of cg2-AG (Figures 2A, 2B and S13). The signal magnitude with 10 μM of cg2-AG was directly comparable to the addition of the CB1 full agonist WIN55 ([WIN55] = 10 μM, n = 84 cells, Figure S13). Addition of cg2-AG only was unable to trigger calcium transients, demonstrating that the coumarin efficiently prevented 2-AG activity (Figure S13G). However, the addition of a preilluminated solution containing cg2-AG triggered a calcium transient similar to the same concentration of 2-AG (Figure S13H and S13I). Release from cg2-AG at internal membranes is likely avoiding premature degradation by the dominantly plasma membrane-bound lipases and could explain the higher potency of 2-AG uncaging over 2-AG addition. Finally, we performed HPLC-MS analysis of lipids extracts prepared from MIN6 cells treated with cg2-AG in the presence or absence of UV light and at two different points in time (30 and 60 min after addition of cg2-AG; see Figure S14). As expected, UV light exposure clearly reduced the amount of cg2-AG in cells. Prolonged incubation times did not reduce the quantity of caged lipid inside cells, confirming that cg2-AG was not significantly metabolized by the cells over time.

Upon activation, CB1 is known to interact with the G-protein inwardly rectifying the potassium channel (GIRK) through the β/γ subunit,[20] triggering opening of the channel and membrane hyperpolarization. Therefore, we performed whole-cell patches in voltage clamp and current clamp mode on MIN6 cells under the same buffer conditions as for the calcium imaging experiments described above (Figure 2C). Before the recording, MIN6 cells were incubated with 10 μM of cg2-AG, added directly to the culture media. After 10 min, the media was replaced with imaging buffer containing 11 mM glucose. In the absence of light, the caged endocannabinoid was unable to activate the potassium channel opening (Figure 2D). UV light irradiation at 375 nm transiently triggered the opening of GIRK channels (Figure 2D, middle panel and 2E), leading to an outward current (13.9 pA ± 3.9, n = 5) that was inhibited with the selective GIRK channel blocker tertiapin (100 nM, 3.2 pA ± 0.4, n = 4, Figure 2D, lower trace and Figure 2G). GIRK opening by the agonist diazoxide served as a positive control (Figure 2D, 2E, upper trace and 2F).

CB1 receptors signal through $G_{i/o}$ protein activation and subsequent inhibition of adenylate cyclase (AC).[21] Alterations of the AC activity has been reported to disrupt the Ca^{2+}-cAMP-PKA oscillatory circuit in MIN6 cells.[22] Therefore, we monitored the inhibition of forskolin-stimulated adenylate cyclase (AC) and protein kinase A (PKA) activity after CB1 activation via cg2-AG uncaging. We used a genetically encoded EPAC-based cAMP sensor[23] and the PKAFRET sensor AKAR4.[24] After 48 h transfection, cells were incubated in the presence or absence of cg2-AG (10 μM), and the culture media was exchanged with 11 mM glucose imaging buffer. After a 10 min resting period, cells were mounted on the microscope (λ_{ex} = 440 nm) and the ratio CFP/YFP was monitored during stimulation with forskolin (50 μM). After flash photolysis, we found a significant reduction in forskolin-induced cAMP levels as well as PKA activation compared to illumination in the absence of cg2-AG (Figure 3A,B,D) (AC inhibition: 27.9% ± 1.4, n = 46 cells, nontreated cells n = 17; PKA inhibition: 19.0% ± 0.9, n = 34 and n = 23, respectively). It is important to note that

cg2-AG showed no fluorescence at 440 nm. Therefore, the caged lipid does not interfere with CFP/YFP-based FRET sensors (Figure 3C).

In summary, we introduced a new strategy allowing for a fully controlled spatiotemporal release of 2-AG in live cells without altering the enzymatic machinery nor using genetic modifications. The mechanism of photorelease allowed for the direct visualization of the uncaging reaction by monitoring the fluorescence emission of the cage. We established proof-of-concept that cg2-AG uncaging is useful to activate CB1 and its downstream effectors in live β-cells.

Supplementary Material

Refer to Web version on PubMed Central for supplementary material.

ACKNOWLEDGMENTS

C.S. is grateful for financial support by OHSU, the EMBL and the Deutsche Forschungsgemeinschaft (TRR186, projects A3 and Z1). M.J.K. recognizes the National Institutes of Health for continued support (NIH grants: R01 NS 038809 and DK 068098).

REFERENCES

(1). Castillo PE; Younts TJ; Chavez AE; Hashimotodani Y. Endocannabinoid signaling and synaptic function. Neuron 2012, 76, 70. [PubMed: 23040807]

(2). Gonsiorek W; Lunn C; Fan X; Narula S; Lundell D; Hipkin RW Endocannabinoid 2-Arachidonyl Glycerol Is a Full Agonist through Human Type 2 Cannabinoid Receptor Antagonism by Anandamide. Mol. Pharmacol 2000, 57, 1045. [PubMed: 10779390]

(3). Piomelli D. The molecular logic of endocannabinoid signalling. Nat. Rev. Neurosci 2003, 4, 873. [PubMed: 14595399]

(4). Bermudez-Silva FJ; Perez JS; Nadal A; de Fonseca FR The role of the pancreatic endocannabinoid system in glucose metabolism. Best Pract. Res. Clin. Endocrinol. Metab. 2009, 23, 87. [PubMed: 19285263]

(5). Ueda N; Tsuboi K; Uyama T; Ohnishi T. Biosynthesis and degradation of the endocannabinoid 2-arachidonoylglycerol. Biofactors 2011, 37, 1. [PubMed: 21328621]

(6). Blankman JL; Simon GM; Cravatt BF A comprehensive profile of brain enzymes that hydrolyze the endocannabinoid 2-arachidonoylglycerol. Chem. Biol 2007, 14, 1347. [PubMed: 18096503]

(7). Jäntti MH; Putula J; Turunen PM; Näsman J; Reijonen S; Lindqvist C; Kukkonen JP Autocrine endocannabinoid signaling through CB1 receptors potentiates OX1 orexin receptor signaling. Mol. Pharmacol 2013, 83, 621. [PubMed: 23233488]

(8). Battista N; DiTommaso M; Bari M; Maccarrone M. The endocannabinoid system: an overview. Front. Behav. Neurosci 2012, 6, 9. [PubMed: 22457644]

(9). Dócs K; Mészár Z; Gonda S; Kiss-Szikszai A; Holló K; Antal M; Hegyi Z. The Ratio of 2-AG to Its Isomer 1-AG as an Intrinsic Fine Tuning Mechanism of CB1 Receptor Activation. Front. Cell. Neurosci 2017, 11, 39. [PubMed: 28265242]

(10). Pan B; Wang W; Long JZ; Sun D; Hillard CJ; Cravatt BF; Liu Q-S Blockade of 2-arachidonoylglycerol hydrolysis by selective monoacylglycerol lipase inhibitor 4-nitrophenyl 4-(dibenzo-[d][1,3]dioxol-5-yl(hydroxy)methyl)piperidine-1-carboxylate (JZL184) Enhances retrograde endocannabinoid signaling. J. Pharmacol. Exp. Ther 2009, 331, 591. [PubMed: 19666749]

(11). Laguerre A; Schultz C. Novel lipid tools and probes for biological investigations. Curr. Opin. Cell Biol 2018, 53, 97. [PubMed: 30015291]

(12). Westphal M; Schafroth MA; Sarott RC; Imhof MA; Bold CP; Leippe P; Dhopeshwarkar A; Grandner JM; Katritch V; Mackie K; Trauner D; Carreira EM; Frank JA Synthesis of Photoswitchable Delta(9)-Tetrahydrocannabinol Derivatives Enables Optical Control of Cannabinoid Receptor 1 Signaling. J. Am. Chem. Soc 2017, 139, 18206. [PubMed: 29161035]

(13). Hoeglinger D; Nadler A; Schultz C. Caged lipids as tools for investigating cellular signaling. Biochim. Biophys. Acta, Mol. Cell Biol. Lipids 2014, 1841, 1085.

(14). Nadler A; Yushchenko DA; Müller R; Stein F; Feng S; Mulle C; Carta M; Schultz C. Exclusive photorelease of signalling lipids at the plasma membrane. Nat. Commun 2015, 6, 10056. [PubMed: 26686736]

(15). glinger D; Haberkant P; Aguilera-Romero A; Riezman H; Porter FD; Platt FM; Galione A; Schultz C. Intracellular sphingosine releases calcium from lysosomes. eLife 2015, 4, No. e10616.

(16). Lin W; Lawrence DS A Strategy for the Construction of Caged Diols Using a Photolabile Protecting Group. J. Org. Chem 2002, 67, 2723. [PubMed: 11950329]

(17). Geißler D; Antonenko YN; Schmidt R; Keller S; Krylova OO; Wiesner B; Bendig J; Pohl P; Hagen W. Coumarin-4-yl)methyl esters as highly efficient, ultrafast phototriggers for protons and their application to acidifying membrane surfaces. Angew. Chem., Int. Ed 2005, 44, 1195.

(18). Li C; Jones PM; Persaud SJ Cannabinoid Receptors are Coupled to Stimulation of Insulin Secretion from Mouse MIN6 β-cells. Cell. Physiol. Biochem 2010, 26, 187. [PubMed: 20798502]

(19). Hegyi Z; Olah T; Kőszeghy A; Piscitelli F; Holló K; Pál B; Csernoch L; Di Marzo V; Antal M. CB1 receptor activation induces intracellular Ca(2+) mobilization and 2-arachidonoylglycerol release in rodent spinal cord astrocytes. Sci. Rep 2018, 8, 10562. [PubMed: 30002493]

(20). Guo J; Ikeda SR Endocannabinoids Modulate N-Type Calcium Channels and G-Protein-Coupled Inwardly Rectifying Potassium Channels via CB1 Cannabinoid Receptors Heterologously Expressed in Mammalian Neurons. Mol. Pharmacol 2004, 65, 665. [PubMed: 14978245]

(21). Hebert-Chatelain E; Desprez T; Serrat R; Bellocchio L; Soria-Gomez E; Busquets-Garcia A; Zottola ACP; Delamarre A; Cannich A; Vincent P; Varilh M; Robin LM; Terral G; García-Fernández MD; Colavita M; Mazier W; Drago F; Puente N; Reguero L; Elezgarai I; Dupuy JW; Cota D; LopezRodriguez ML; Barreda-Gómez G; Massa F; Grandes P; Bénard G; Marsicano G. A cannabinoid link between mitochondria and memory. Nature 2016, 539, 555. [PubMed: 27828947]

(22). Ni Q; Ganesan A; Aye-Han N-N; Gao X; Allen MD; Levchenko A; Zhang J. Signaling diversity of PKA achieved via a Ca2+-cAMP-PKA oscillatory circuit. Nat. Chem. Biol 2011, 7, 34. [PubMed: 21102470]

(23). Klarenbeek J; Goedhart J; van Batenburg A; Groenewald D; Jalink K. Fourth-generation epac-based FRET sensors for cAMP feature exceptional brightness, photostability and dynamic range: characterization of dedicated sensors for FLIM, for ratiometry and with high affinity. PLoS One 2015, 10 (4), No. e0122513.

(24). Depry C; Allen MD; Zhang J. Visualization of PKA activity in plasma membrane microdomains. Mol. BioSyst 2011, 7, 52. [PubMed: 20838685]

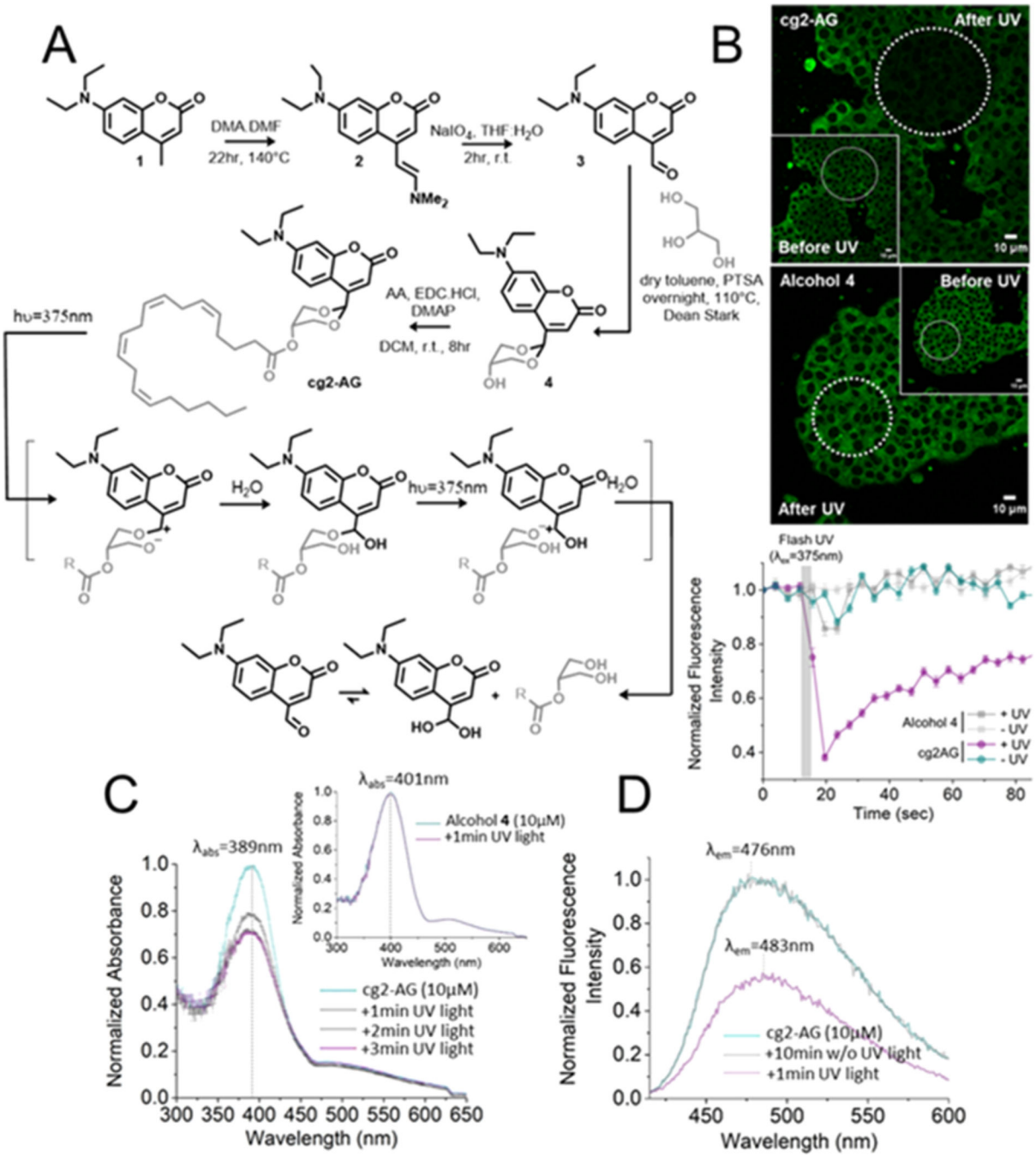

Figure 1.

(A) Chemical synthesis of caged 2-arachidonoylglycerol (cg2-AG) and proposed solvent-assisted mechanism of photorelease. (B) Confocal micrographs of live MIN6 treated with 10 μM cg2-AG or alcohol **4**, before and after flash photolysis in a circular region of interest (λ_{ex} = 405 nm, $\lambda_{uncaging}$ = 375 nm). Normalized fluorescence intensity of live MIN6 cells treated with cg2-AG (10 μM) or alcohol **4** in ± UV. The reduction in fluorescence after photolysis is likely due to (C) UV/vis spectra of cg2-AG (10 μM in H_2O) ± UV light photolysis (from 1 to 3 min irradiation, 1 kW xenon lamp equipped with a 350 nm long-pass

filter). Top right inlet. UV/vis spectra of alcohol **4** under the same conditions is not affected by the presence of light. (D) Fluorescence emission spectra of cg2-AG (10 μM in H_2O, λ_{ex} = 405 nm), ± UV light photolysis.

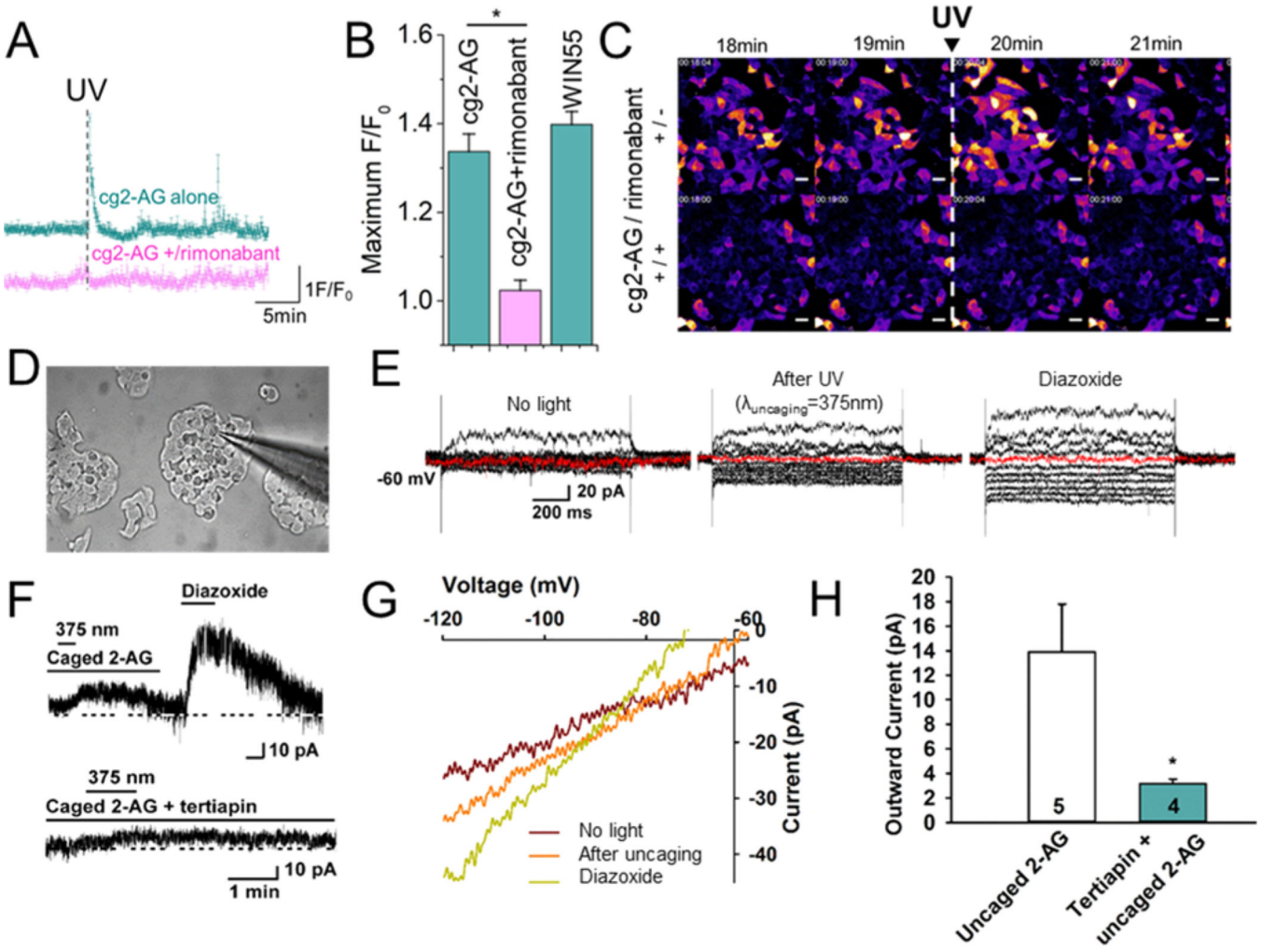

Figure 2.

(A) Representative traces of fluorescence increase F/F_0 of live MIN6 cells pretreated with the cell permeant calcium dye Fluo4/AM (5 μM) in the presence of cg2-AG ([cg2-AG] = 10 μM, n = 6, cyan trace) and subjected to flash photolysis (λ_{ex} = 488 nm, $\lambda_{uncaging}$ = 375 nm) with and without the CB1 antagonist rimonabant (1 μM; [cg2-AG] = 10 μM, n = 6, pink trace). (B) Bar graphs summarizing fluorescence intensity increase F/F_0 of the calcium dye Fluo4/AM (5 μM) in MIN6, treated with cg2-AG and subjected to flash photolysis in the absence ([cg2-AG] = 10 μM, n = 136) or presence of rimonabant (1 μM; [cg2-AG] = 10 μM, n = 79). The CB1 agonist WIN55 was used as a positive control ([WIN55] = 10 μM, n = 84). (C) Calcium imaging of MIN6 cells upon the uncaging of cg2-AG (10 μM) ± preincubation with rimonabant (1 μM). (D) Photomicrograph showing a recording pipet patched onto a MIN6 cell dispersed on a coverslip. (E) Currents generated in a whole-cell recording of a MIN6 cell elicited by holding the cell at −60 mV and giving a series of 1 s prepulses ranging from −50 mV to −140 mV (in 10 mV increments) and stepping back to −60 mV before, after photostimulation (0.6 mW for 1 min, and during perfusion with 300 μM diazoxide). (F) Representative traces of photoinduced currents by released 2-AG, K_{ATP} opener diazoxide, or GIRK channel blocker tertiapin (upper trace). After a seal was formed and the whole-cell

configuration was obtained, cells were perfused with cg2-AG (10 μM) for 10 min before activating with a 375 nm light pulse. After the current returned to resting level, the cells were perfused with diazoxide, which generated a robust outward current. V_{hold} = −60 mV (lower trace). The outward current induced by the uncaging of cg2-AG was blocked by pretreatment with GIRK channel blocker tertiapin (100 nM) for 15 min. (G) *I/V* curves generated in MIN6 cells in the presence of cg2-AG (10 μM, ± UV light) or diazoxide (300 μM). (H) Bar graphs summarizing the effects of cg2-AG in absence or presence of tertiapin. Data points represent the mean ± SEM. Cell numbers are indicated. Unpaired *t* test, $t = 2.551$, $P = 0.0447$.

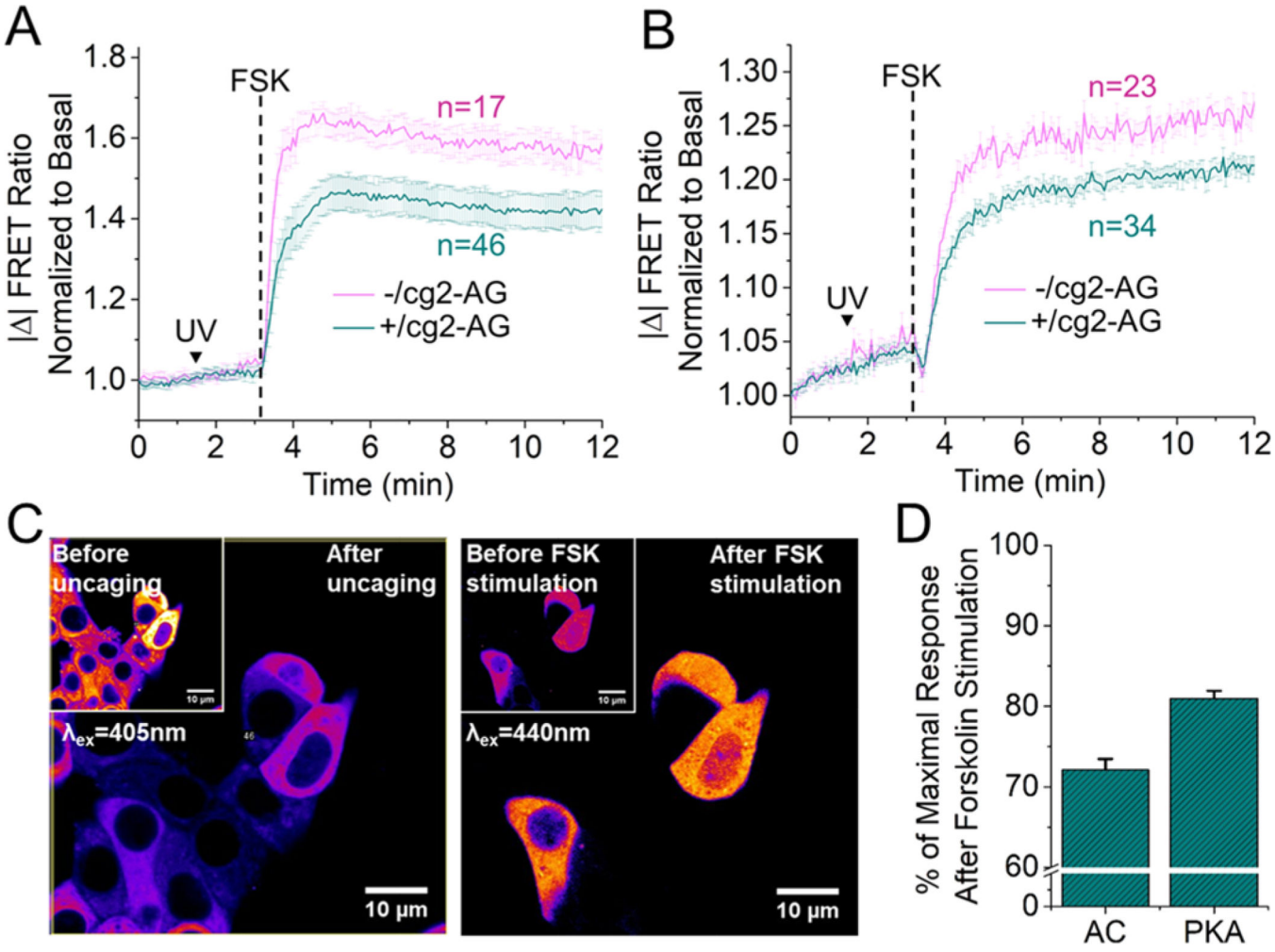

Figure 3.

Normalized FRET change ratio of the genetically encoded EPAC-based cAMP sensor (A) and the A-kinase FRET sensor AKAR4 (B) in MIN6 cells upon stimulation with forskolin (FSK, 50 μM), in presence or absence of cg2-AG (10 μM). (C) Fluorescence emission of cg2-AG before and after photouncaging (left panel) and FRET ratio change of the EPAC-based sensor, before and after stimulation with FSK (50 μM, right panel). (D) Bar graphs summarizing CB1-mediated inhibition of adenylate cyclase and protein kinase A activity upon cg2-AG uncaging.